

Universal quark-jet fragmentation in soft hadronic reactions

Hisakazu Minakata*

Department of Physics, Tokyo Metropolitan University, Setagaya, Tokyo 158, Japan

(Received 19 March 1979)

We present a parton model describing all the parts of nondiffractive small- p_{\perp} particle production on the basis of (i) quantum-chromodynamics inspired multijet view, (ii) universality of quark-jet hadronization, and (iii) correspondence arguments to dual Regge models. The model reproduces well, without any adjustable parameters, experimental data on average multiplicities and meson distributions in the fragmentation region of mesons and in $\bar{p}p$ annihilation. We argue that the quark-recombination mechanism of Das and Hwa is incorporated in our model in the form of a nonvanishing quark decay function $D(z)$ at $z \rightarrow 1$. A new test of the multijet point of view is also proposed.

I. INTRODUCTION

The parton model¹ has been applied to various hard processes and enjoys amazing success. Recently it was shown that the perturbative treatment of quantum chromodynamics (QCD) provides a firm basis for the parton description of hard processes.² It is of considerable interest to ask to what extent such parton description can be extended to soft hadronic reactions.

To answer the question, however, is not an easy task because some nonperturbative effects may play an important role there. We present in this paper an attempt to give an answer by proposing a parton model which describes all parts of small- p_{\perp} nondiffractive particle production. Lacking a reliable method for treating the nonperturbative effects, we choose to follow a unifying aspect of gauge and dual theories.³

Our guiding principles in the present approach are as follows:

(i) $1/N_c$ expansions of 't Hooft⁴ and/or Veneziano⁵ and the multijet structure of hadronic final states inspired by these viewpoints.

(ii) Universality of quark-jet hadronization in soft as well as hard reactions.

(iii) Correspondence to dual Regge models, especially, to dual topological unitarization (DTU).⁵

The quark-parton-model approach to soft hadronic reactions already started some time ago.^{1,6} Bjorken and Kogut⁷ introduced the notion of correspondence. The universal behavior of the average multiplicity was incorporated into the wee-quark-exchange model of Brodsky and Gunion.⁸ More recently, Ochs⁹ noted a similarity between particle ratios in large- and small- p_{\perp} reactions. This similarity has been cast into several different models,¹⁰⁻¹³ according to their own points of view. Among them, the recombination model of Das and Hwa¹⁰ has attracted much interest.

Our approach differs from those mentioned above mainly in the following two aspects: One is the inclusion of the hierarchy of various processes by the number of jets consisting in hadronic final states. The other is that our approach aims to treat all parts of nondiffractive small- p_{\perp} particle production, unlike the models restricted to the fragmentation region. Because of the latter property our model can predict not only the shape but also the absolute magnitude of the single-particle cross sections. Moreover, we shall argue that the quark-recombination mechanism is included at least partly in our model after taking the differences stated above into account.

In Sec. II, we present a possible interpretation of multijet structure from the parton-model viewpoint and set up the dressed-quark model. In the following sections, we will compare our model with the experimental data on average multiplicities (Sec. III), meson distributions in the fragmentation region of mesons (Sec. IV), and in $\bar{p}p$ annihilation (Sec. V). In Sec. VI we will discuss the relation between our dressed-quark decay and the quark-recombination mechanisms. The last section will be devoted to conclusion and discussion, in which we propose a new test of the multijet point of view.

II. DRESSED-QUARK MODEL

A. The model

In the QCD-inspired multijet view,³ the hadronic final states of e^+e^- , hadron-hadron (nonannihilation), and baryon-antibaryon annihilation processes dominantly consist, respectively, of one, two, and three sheets (jets)¹⁴ of hadrons. We take the following picture: Each production sheet can be regarded in its forward (backward) hemisphere as if a valence quark in the projectile (target) is decaying into a cascade jet of hadrons (see Fig. 1). The

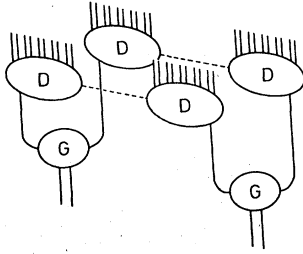


FIG. 1. Schematic illustration of hadronic particle production in two-sheet processes.

decaying quarks, however, are not identical with the ones in the usual parton description of deep-inelastic or large- p_{\perp} processes. This is because, in our case, the quarks should carry the whole momentum of hadrons, whereas in the latter case the quarks are expected to have only a certain fraction of parent momentum, e.g., 50% for the proton. Therefore, the decaying quarks in our case should be interpreted as dressed valence quarks including therein the whole effects of gluons and sea quarks. The notion of dressed quarks as a "cluster" of partons has been proposed by several authors.¹⁵ It may also have an intimate connection with the valence-quark approximation¹⁶ as a generalization of the Kogut-Susskind picture¹⁷ to the small- Q^2 region.

Now we are led to the picture that in the forward (backward) hemisphere, the beam (target) meson first breaks up into the dressed valence quark and antiquark, and subsequently they decay into jets of hadrons (see Fig. 1). In the description of baryon fragmentation, the antiquark in the meson case should be replaced by a diquark. In the case of baryon-antibaryon annihilation, the baryon (and also antibaryon) is assumed to break up into three valence quarks and they convert into hadronic jets.

In formulating the model we exploit the light-cone fraction instead of Feynman's variable because it makes the separation of the forward and backward hemispheres boost invariant. The inclusive single-particle distribution of hadron c (integrated over transverse momentum) in the forward hemisphere of hadron a can be written as

$$\frac{1}{\sigma} x \frac{d\sigma}{dx} = \sum_i \int_x^1 dx' G_{a \rightarrow i}(x') \left(\frac{x}{x'} \right) D_{i \rightarrow c} \left(\frac{x}{x'} \right), \quad (2.1)$$

where $G_{a \rightarrow i}$ denotes the dressed i -quark distribution inside the hadron a and $D_{i \rightarrow c}$ is the decay function of the dressed i quark to the hadron c . The summation in (2.1) runs over the valence quarks designated before in each reaction. In spite of the fact that a production sheet is formed between quarks in the projectile and target, the distribution in the forward hemisphere is not affected by

the quark distribution in the target, and vice versa. This is due to the use of the light-cone fraction $x = (E + p_{\parallel}) / \sqrt{s}$. This property also means that no forward-backward correlations are generated through the mechanism of energy-momentum partition to sheets. This is in sharp contrast with the prediction from the counting-rule argument¹⁸ where the mismatch of the quantum number implies a strong forward-backward correlation.

Now let us proceed to the determination of dressed-quark distributions and decay functions.

B. Dressed-quark distribution

We go back from the usual parton stage to the dressed-quark stage which we have assumed to be relevant to low-momentum transfer hadronic reactions. Hereafter we denote the former parton as the bare one. We propose that the quark distributions in these two stages are connected to each other by a relation

$$\int_x^1 \frac{dx'}{x'} G(x') F(x/x') = f(x), \quad (2.2)$$

which is similar to the one connecting different stages of matter in the Kogut-Susskind picture.¹⁷ In (2.2), f denotes the bare valence-quark distribution and F is the fragmentation function of the dressed quark to bare valence quarks. Here we have assumed the flavor independence of G and suppressed flavor indices.

We use a heuristic method to determine G from knowledge of f . For brevity, we assume the power form of G , F , and f :¹⁹

$$\begin{aligned} G(x) &= \frac{1}{B(\alpha+1, \beta+1)} x^{\alpha} (1-x)^{\beta}, \\ F(x) &= \frac{1}{B(\alpha'+1, \beta'+1)} x^{\alpha'} (1-x)^{\beta'}, \\ f(x) &= \frac{1}{B(\gamma+1, \delta+1)} x^{\gamma} (1-x)^{\delta}, \end{aligned} \quad (2.3)$$

where $B(x, y)$ is the Euler beta function. Under (2.3), consistent solutions can easily be found by projecting the equation into moment space. We obtain

$$\begin{aligned} \text{Solution (a)} \quad & \alpha = \gamma, \quad \alpha' = \gamma + \beta + 1, \quad \beta' = \delta - \beta - 1. \\ \text{Solution (b)} \quad & \alpha' = \gamma, \quad \alpha = \gamma + \beta' + 1, \quad \beta = \delta - \beta' - 1. \end{aligned} \quad (2.4)$$

It should be noticed that the dressed-quark distribution in the meson should have the form

$$\begin{aligned} G_M(x) &= \frac{1}{B(\alpha_M+1, \alpha_M+1)} \int_0^1 dy (xy)^{\alpha_M} \delta(1-x-y) \\ &= \frac{1}{B(\alpha_M+1, \alpha_M+1)} x^{\alpha_M} (1-x)^{\alpha_M}, \end{aligned} \quad (2.5)$$

namely, $\beta = \alpha = \alpha_M$. Further, we assume the following form of G for the baryon:

$$G_B(x) = \frac{\Gamma(3\alpha_B + 3)}{\Gamma(\alpha_B + 1)^3} \int_0^1 dy dz (xyz)^{\alpha_B} \delta(1 - x - y - z) \\ = \frac{1}{B(\alpha_B + 1, 2\alpha_B + 2)} x^{\alpha_B} (1 - x)^{2\alpha_B + 1}, \quad (2.6)$$

which is consistent with (2.3) with $\alpha = \alpha_B$ and $\beta = 2\alpha_B + 1$. In other words, quarks are assumed to be uncorrelated apart from the effect of momentum conservation.

We reasonably require the following conditions on the exponents in the bare valence-quark distributions:

$$\gamma_M = \gamma_B = -\alpha_r(0) \simeq -\frac{1}{2}, \quad (2.7) \\ 0 \leq \delta_M \leq 1, \quad 3 \leq \delta_B \leq 4,$$

where $\alpha_r(0)$ stands for the intercept of the meson Reggeon. The first condition in (2.7) comes from the continuity argument between the scaling and Regge regions,¹ the second implies a region between two theoretical values,^{20,21} and the third is a tentative representation of the experimental value.

Under (2.7) the exponents in G and F are constrained as

$$\alpha_M = \alpha_B = -\alpha_r(0) = -\frac{1}{2}, \quad \alpha'_M = 0, \quad -\frac{1}{2} \leq \beta'_M \leq \frac{1}{2}, \\ \alpha'_B = \frac{1}{2}, \quad 2 \leq \beta'_B \leq 4 \quad (2.8)$$

for solution (a) and

$$-\frac{1}{4} \leq \alpha_M \leq \frac{1}{4}, \quad \alpha'_M = \alpha'_B = -\frac{1}{2}, \quad -\frac{3}{4} \leq \beta'_M \leq -\frac{1}{4}, \\ \frac{1}{2} \leq \alpha_B \leq \frac{5}{6}, \quad 0 \leq \beta'_B \leq \frac{1}{3} \quad (2.9)$$

for solution (b).

We choose solution (a) because of the universal value of α for meson and baryon cases. This is also supported by the following argument based on the correspondence to dual-Regge models.

We restrict ourselves to the meson-meson collisions (dominantly two-sheets). The partition of energy and momentum to each sheet is controlled by the dressed-quark distribution G . As a measure of it, we calculate the scaled sheet mass distribution,

$$\rho(u, v) = \int_0^1 dx_1 dx_2 G_M(x_1) G_M(x_2) \delta(u - x_1 x_2) \\ \times \delta(v - (1 - x_1)(1 - x_2)), \quad (2.10)$$

where $u = s_1/s$, $v = s_2/s$, and $s_i(s)$ is the c.m. system energy squared of sheet i (colliding hadrons). Taking (2.5) for G_M , we have

$$\rho(u, v) = \frac{2}{B(\alpha + 1, \alpha + 1)^2} \frac{(uv)^\alpha}{\{1 - 2(u+v) + (u-v)^2\}^{1/2}}. \quad (2.11)$$

It should be noticed that the form (2.11) exactly coincides with the common piece of the "sheet-mass" distribution of the dual resonance and dual multiperipheral models under the choice $\alpha = -\alpha_r(0)$,²² i.e., solution (a).

The intuitive meaning of solution (a) is clear. Since the behavior of the quark distributions at $x \simeq 0$ is stable through the fragmentation process, $x^{-\alpha_r(0)}$ behavior should be initiated in the dressed-quark distributions. The exponents at $x \simeq 1$ are determined by kinematic constraint and differ in meson and baryon cases.

The negative value of α implies that the dressed quarks in hadrons live in a rather asymmetric configuration, one fast and the other slow. Andersson *et al.*¹¹ discussed an extreme case in which one of the quarks had a whole momentum of the hadron. However, there was no theoretical justification in their treatment. The asymmetry of sheet size originating in this asymmetry of quark momentum configuration is shown to be important in reducing the slope ratio $\alpha'_{\text{pomeron}}/\alpha'_{\text{Reggeon}}$ down from the standard value $\frac{1}{2}$.²³

C. Dressed-quark decay function

We assume that the decay function of the dressed quark has the same form as that of the bare quark. This assumption is quite natural in the multijet point of view motivated by the $1/N_c$ expansion of QCD.³

Another aspect of this assumption is that it may be the case if the jet hadronization occurs as a consequence of confinement mechanism as in two-dimensional QED.²⁴ In this theory the fast-separating quarks are treated as c -number currents. Therefore, the particle production should be insensitive to the nature of these quarks, i.e., dressed or bare, as far as such treatment is relevant. In this respect Satz²⁵ emphasized that the quark distributions should be modified, whereas the decay functions are universal in soft hadronic reactions.

Now our model is completely specified in a form without any adjustable parameters.

III. AVERAGE MULTIPLICITY

Let us examine to what extent our model can describe the experimental data. The first hurdle for the multijet point of view is the fact that the average multiplicity in $\bar{p}p$ annihilation has the same order of magnitude as that in e^+e^- annihilation, despite three times the number of sheets.

The generating function of the multiplicity distribution for three-sheet processes can be expressed as

$$F^{(3)}(s, h) = \left(\frac{\Gamma(3\alpha + 3)}{\Gamma(\alpha + 1)^3} \right)^2 \int_0^1 \prod_{i=1}^3 dx_i dy_i (x_i y_i)^{\alpha} F^{(1)}(s x_i y_i, h) \delta \left(1 - \sum_{i=1}^3 x_i \right) \delta \left(1 - \sum_{i=1}^3 y_i \right), \quad (3.1)$$

where $F^{(1)}(s_i, h)$ stands for the generating function for each sheet with mass squared s_i and x 's and y 's are the momentum fractions of dressed quarks. Here we have assumed the absence of correlations among sheets, apart from the one introduced by energy-momentum conservation.

For simplicity and clarity, we adopt the Poisson distribution for the multiplicity distribution in each sheet and assume the logarithmic multiplicity

$$F^{(1)}(s, h) = e^{h\langle n(s) \rangle}, \quad (3.2)$$

$$\langle n(s) \rangle = a \ln s + b. \quad (3.3)$$

The generating function for three-sheet processes is then given by

$$F^{(3)}(s, h) = e^{3h(a \ln s + b)} \times \left[\frac{\Gamma(\alpha + ah + 1)^3}{\Gamma(3\alpha + 3ah + 3)} \frac{\Gamma(3\alpha + 3)}{\Gamma(\alpha + 1)^3} \right]^2. \quad (3.4)$$

Although the integration in (3.1) extends over the unphysical region $x_i y_i \lesssim s_0/s$ (s_0 is the lowest value of sheet mass squared), it can be shown that the contribution from the region is negligible provided that $s_0/s \ll 1$ and α is not very near to -1 . Now it is straightforward to calculate the average multiplicity and correlation moments. We have

$$\langle n(s) \rangle^{(3)} = 3\langle n(s) \rangle^{(1)} + 6a\psi(\alpha + 1) - 6a\psi(3\alpha + 3), \quad (3.5)$$

$$f_2^{(3)} = 6a^2\psi'(\alpha + 1) - 18a^2\psi'(3\alpha + 3), \quad (3.6)$$

etc., where ψ and ψ' are digamma and trigamma functions, respectively.

It should be noticed that our result (3.5) of the average multiplicity is valid *irrespective* of the form of input multiplicity distribution. It is solely the consequence of the three-sheet structure (3.1) and logarithmic multiplicity (3.3). Because of this property and of the independence of the multiplicity of the decay function, this is one of the best quantities to test our choice of the dressed-quark distribution function.

On the other hand, the correlation moments depend on the input distributions. However, it is noticeable that our mechanism of energy-momentum partition to sheets does not introduce any long-range order correlations.

The average multiplicities in meson-meson, meson-baryon, and baryon-baryon collisions (two sheets) can be obtained in an analogous way. The results are

$$\langle n(s) \rangle_{MM}^{(2)} = 2\langle n(s) \rangle^{(1)} + 4a\psi(\alpha + 1) - 4a\psi(2\alpha + 2), \quad (3.7)$$

$$\langle n(s) \rangle_{MB}^{(2)} = 2\langle n(s) \rangle^{(1)} + 3a\psi(\alpha + 1) - a\psi(2\alpha + 2) - 2a\psi(3\alpha + 3), \quad (3.8)$$

$$\langle n(s) \rangle_{BB}^{(2)} = 2\langle n(s) \rangle^{(1)} + 2a\psi(\alpha + 1) + 2a\psi(2\alpha + 2) - 4a\psi(3\alpha + 3). \quad (3.9)$$

In Fig. 2, we plot the model predictions on average multiplicities in meson-meson, meson-baryon, baryon-baryon, and baryon-antibaryon annihilation reactions. As an input we use the multiplicity in e^+e^- reactions fitted by²⁶

$$\langle n(s) \rangle^{(1)} = 0.65 \ln s + 2.3. \quad (3.10)$$

Before entering into the comparison with data, it should be noticed that our model deals only with the nondiffractive part of particle production. Therefore the plotted data on the $p\bar{p}$ interaction cannot be compared directly with our prediction.

Our prediction on $p\bar{p}$ annihilation with $\alpha = -\alpha_r(0) = -\frac{1}{2}$ agrees reasonably well with the experimental value. The multiplicity is so sensitive to α that even the choice $\alpha = 0$ fails to describe the data as seen from Fig. 2. Also the fact that our prediction on the baryon-baryon case lies above the $p\bar{p}$ data is consistent with our earlier comment, since the

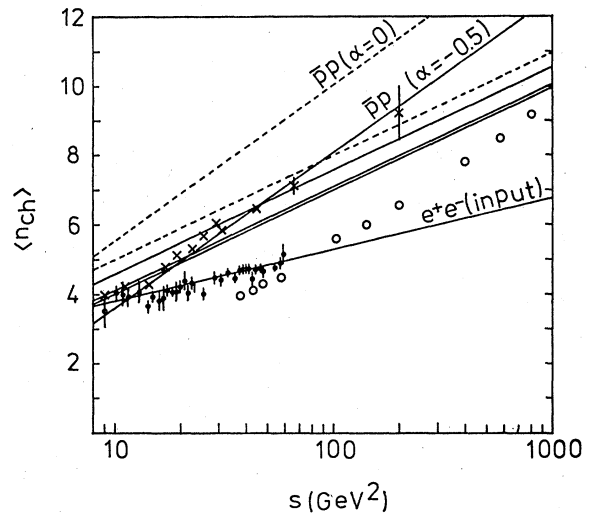


FIG. 2. The average charged multiplicities in e^+e^- annihilation (\bullet), $p\bar{p}$ interaction (\circ), and in $p\bar{p}$ annihilation (\times) (Ref. 26). The solid lines denote, from above at large s , our model predictions for $p\bar{p}$ annihilation, baryon-baryon, meson-baryon, and for meson-meson collisions. The fit to the data of e^+e^- annihilation is the input Eq. (3.10). Also shown (dashed lines) are the results with $\alpha = 0$ for $p\bar{p}$ annihilation and baryon-baryon collisions, where the latter is equal to the ones of meson-baryon and meson-meson collisions.

diffractive component is expected to have smaller multiplicity than the nondiffractive one.

The origin of the large subtraction term in two- and three-sheet multiplicities is due to the asymmetry of sheet size. Since the logarithmic multiplicity is slowly varying at large sheet mass, the asymmetry of sheet size diminishes the effective number of sheets.

IV. MESON FRAGMENTATION

Encouraged by the success in describing the average multiplicity, we attempt a systematic comparison of the prediction on inclusive single-particle distributions with experimental data. We treat the meson fragmentation in the present Section and the $\bar{p}p$ annihilation in the next Section. We postpone the discussion of baryon fragmentation to another occasion since it requires the knowledge of diquark decay functions.

The choice $\alpha = -\frac{1}{2}$ and the assumption of flavor independence of G completely determine all the dressed-quark distributions. For the decay functions, we use the parametrization by Field and Feynman,²⁷ or more precisely, the one with analytic approximation introduced by them. Putting them into (2.1), we can compute all the meson-meson distributions where the meson implies any of π^\pm , π^0 , K^\pm , or K_S . The absolute normalization is fixed by multiplying the nondiffractive inelastic cross section. Lacking the knowledge of the diffractive inelastic cross section, we simply assume it to be set equal to the elastic cross section. This assumption is approximately satisfied in pp collision.

It is, if possible, desirable that experimental data with incident laboratory momentum larger than 100 GeV/c are selected to compare with our predictions. This energy corresponds to the mean c.m.s. energy of a sheet ~ 7 GeV where the jet structure is cleanly developed in the e^+e^- annihilation process.

In Fig. 3 we compare our model with the data on the π^\pm distribution in the fragmentation region²⁸ of π^\mp at laboratory momentum 100 GeV/c.^{29,30} The data are plotted as a function of Feynman's variable, not the light-cone fraction. Therefore the comparison at too small x (say $x \leq 0.1$) does not have a serious meaning. For the sake of comparison we plot also the case with $\alpha = +0.5$. (The case of $\alpha = 0$ is roughly the mean.) Though the α dependence is relatively mild, the behavior at large x shows a deviation in favor of the negative value of α .

As a possible origin of the discrepancy at large x , we consider the diffractive dissociation $\pi^\pm \rightarrow A_1^\pm \rightarrow \pi^\mp(\pi^\pm\pi^\pm)$. We borrow the estimate given in Ref. 32

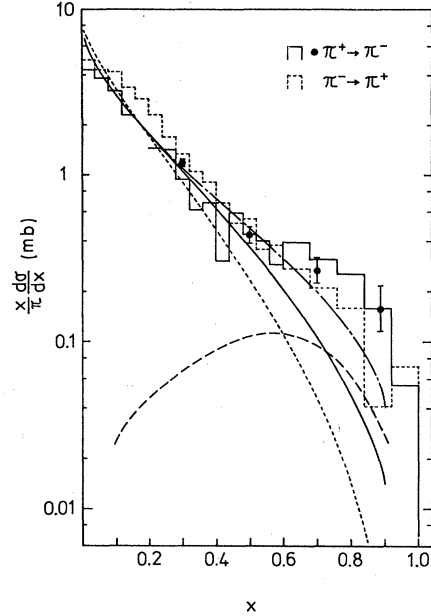


FIG. 3. The inclusive π^\pm distributions integrated over p_1 in the fragmentation regions of π^\mp . The solid ($\pi^+ \rightarrow \pi^-$) and dotted ($\pi^- \rightarrow \pi^+$) histogram are the data at 100 GeV/c in Ref. 29. The data on the π^+ distribution in Ref. 30 are also shown. The solid and dash-dot curves are our model predictions without and with the contribution from diffraction (represented by dashed curve), respectively. The nondiffractive inelastic cross sections are fixed as 17 mb for both π^+p and π^-p reactions (see text). For elastic cross sections, see Ref. 31. The case with $\alpha = +0.5$ (without diffraction) is also plotted by a dotted curve for comparison.

and plot in the same figure the prediction taking into account this component. The fit is appreciably improved.

In Fig. 4, the π^+ and K^+ distributions in the fragmentation region of π^+ at 100 GeV/c (Ref. 30) are plotted together with our theoretical curves. The diffractive component is subtracted in the data on the π^+ distribution by parametrizing it in terms of the triple-Regge form.³⁰ Although it corresponds theoretically to nucleon diffraction, some part of pion diffraction may also be subtracted by this procedure. Thus we do not include the diffractive component into the model prediction in Fig. 4.

It is remarkable that our model can reproduce the $\pi^+ \rightarrow K^+$ spectrum rather well. Notice that the absolute normalization of the curve is the prediction. This feature contrasts with the case of Andersson *et al.*'s model.³⁰ A precise measurement at lower x can be a clean test of our model.

Figure 5 includes the π^+ and π^- distribution in the fragmentation region of K^+ at 100 (Ref. 30) and 70 GeV/c,³³ respectively. We see that our model can fit the data well. It is, however, inconclusive

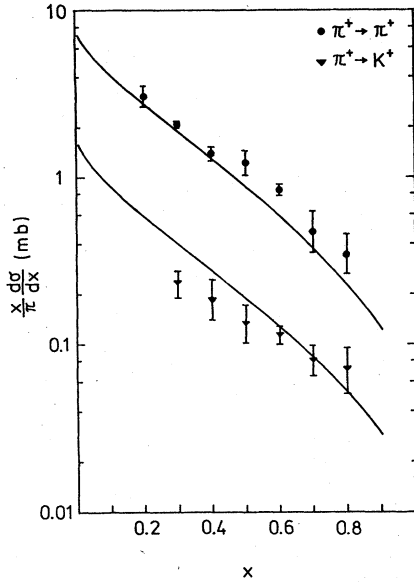


FIG. 4. The inclusive π^+ (\bullet) and K^+ (\blacktriangledown) distributions integrated over p_{\perp} in the fragmentation region of π^+ at 100 GeV/c (Ref. 30). The solid curves are our model predictions.

for the π^+ distribution since the data have error bars which are too large.

For systematic comparison, we plot in Fig. 6 all the normalized meson \rightarrow meson distributions. The slow decrease of the K^+ distributions in the fragmentation regions of K^+ and π^+ is quite eminent. This is mainly due to the slow falloff of the decay function $D_{u \rightarrow K^+}$.

V. BARYON-ANTIBARYON ANNIHILATION

The meson spectra in baryon-antibaryon annihilation can be calculated similarly, using (2.6) and the Field-Feynman decay functions. Unfortunately, however, there is no genuine annihilation data at sufficiently high energies (~ 220 GeV/c under the same criterion as before). Therefore we compare our model with the data at 12 GeV/c.³⁴ The normalized pion distribution of the data is consistent with the onset of scaling in the central region compared with the data on the $\bar{p}p - p\bar{p}$ difference at 100 GeV/c.³⁵

In Figs. 7 and 8, our model predictions are compared with the data on $\bar{p} \rightarrow \pi^+$ ($p \rightarrow \pi^-$) and $\bar{p} \rightarrow \pi^-$ ($p \rightarrow \pi^+$), respectively. Again the case with $\alpha = +0.5$ is also plotted for comparison. It is clear that the negative value of α is definitely favored. The agreement is fairly good for the unfavored-charge pions ($\bar{p} \rightarrow \pi^+$ or $p \rightarrow \pi^-$) whereas it is not so good for favored-charge pions. The discrepancy in the latter case may or may not be due to the low-ener-

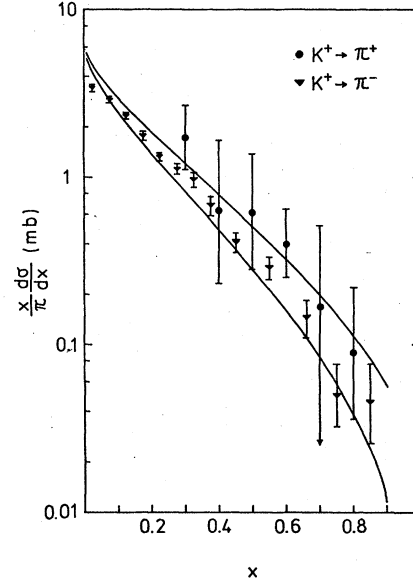


FIG. 5. The inclusive π^+ (\bullet) and π^- (\blacktriangledown) distributions in the fragmentation region of K^+ in K^+p collisions at 100 GeV/c (Ref. 30) for π^+ and 70 GeV/c (Ref. 33) for π^- . The solid curves show our model predictions of, from above, π^+ and π^- distributions. The nondiffractive inelastic cross section is estimated as ≈ 14 mb at both energies. For elastic cross sections, see Ref. 31.

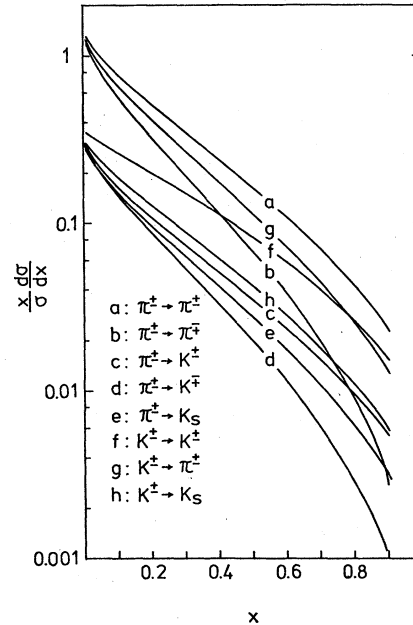


FIG. 6. The normalized meson distributions in fragmentation region of mesons: (a) $\pi^{\pm} \rightarrow \pi^{\pm}$, (b) $\pi^{\pm} \rightarrow \pi^{\mp}$, (c) $\pi^{\pm} \rightarrow K^{\pm}$, (d) $\pi^{\pm} \rightarrow K^{\mp}$, (e) $\pi^{\pm} \rightarrow K_S$, (f) $K^{\pm} \rightarrow K^{\pm}$, (g) $K^{\pm} \rightarrow \pi^{\pm}$, (h) $K^{\pm} \rightarrow K_S$. The distributions $\pi^{\pm} \rightarrow \pi^0$, $K^{\pm} \rightarrow K^{\mp}$, and $K^{\pm} \rightarrow \pi^{\mp}$ are roughly the same as that of $K^{\pm} \rightarrow \pi^{\pm}$ (g), $\pi^{\pm} \rightarrow K^{\mp}$ (d), and $\pi^{\pm} \rightarrow \pi^{\mp}$ (b), respectively. The accuracy of agreement is within $\sim 5\%$ at $x \geq 0.5$.

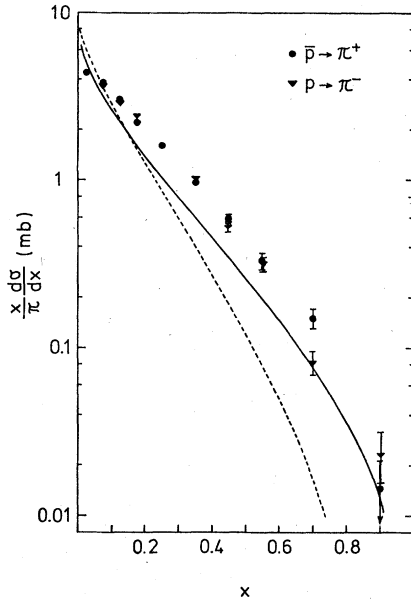


FIG. 7. The inclusive π^+ (π^-) distribution integrated over p_{\perp} in \bar{p} 's (p 's) forward hemisphere in $\bar{p}p$ annihilation in 12 GeV/c (Ref. 34). The solid curve represents our model prediction with annihilation cross section ≈ 12 mb (Ref. 34). Also shown (dotted curve) is the result with $\alpha = +0.5$.

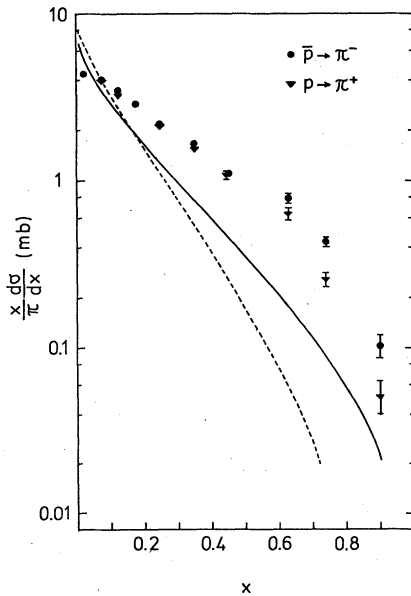


FIG. 8. The inclusive π^- (π^+) distribution in \bar{p} 's (p 's) forward hemisphere in $\bar{p}p$ annihilation at 12 GeV/c (Ref. 34). The solid and dotted curves are our prediction with $\alpha = -0.5$ and the case with $\alpha = +0.5$, respectively.

gy effects.

We show in Fig. 9 all the meson distributions in the $\bar{p}p$ annihilation process for further tests of our model. The K^- distribution in the fragmentation region of the antiproton shows the slowest decrease among them for the same reason as for K^+ in the meson case. The data on meson distributions at higher energies are awaited since they provide a definite test of our model, because of the absence of diffraction in annihilation processes.

VI. DRESSED-QUARK DECAY vs RECOMBINATION

We turn to the problem of clarifying the connection between our model and the quark-recombination picture originally proposed by Das and Hwa¹⁰ and reformulated recently by Hwa and Robert.³⁶ Since our model is so constructed as to describe whole parts of nondiffractive small- p_{\perp} particle production, and since the quark recombination should ultimately be responsible for the hadronization in the quark-parton picture, our model should contain this mechanism in its relevant kinematic region.

We start from the expression of the single-particle distribution in Ref. 36

$$\frac{1}{\sigma} x \frac{d\sigma}{dx} = \int_0^1 \frac{dx_1}{x_1} \frac{dx_2}{x_2} \bar{f}_v(x_1) \bar{f}_s(x_2) \times \rho(x_1, x_2) R(x_1, x_2, x), \quad (6.1)$$

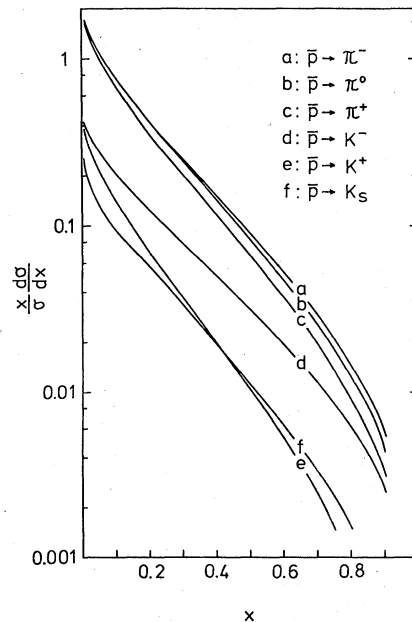


FIG. 9. The normalized meson distributions in $\bar{p}p$ annihilation: (a) $\bar{p} \rightarrow \pi^-$, (b) $\bar{p} \rightarrow \pi^0$, (c) $\bar{p} \rightarrow \pi^+$, (d) $\bar{p} \rightarrow K^-$, (e) $\bar{p} \rightarrow K^+$, (f) $\bar{p} \rightarrow K_S$.

where \tilde{f}_v (\tilde{f}_s) denotes the bare valence quark (sea antiquark) distribution, ρ is a function reflecting the wave function of the wee valence parton, and R describes the recombination probability. In this section we use the quark distributions \tilde{f} with invariant normalization, i.e., $\tilde{f}(x) = xf(x)$ following Ref. 36. Equation (2.2) holds also for the quantities with tildes.

Using Eq. (2.2) with tildes and changing the order of integration, we can rewrite (6.1) into the form

$$\frac{1}{\sigma} x \frac{d\sigma}{dx} \int_0^1 d\xi G(\xi) \left(\frac{x}{\xi}\right) D(x, \xi), \quad (6.2)$$

where

$$D(x, \xi) = \left(\frac{\xi}{x}\right) \int_0^\xi \frac{dx_1}{x_1} \tilde{F}(x_1/\xi) \times \int_0^1 \frac{dx_2}{x_2} f_s(x_2) \rho(x_1, x_2) R(x_1, x_2, x). \quad (6.3)$$

If the function D scales, i.e., $D = D(x/\xi)$, it can be interpreted as a dressed-quark decay function in our model.

Now we restrict ourselves to the meson fragmentation since our model is not yet fully specified to treat the baryon fragmentation. We take as in Ref. 36

$$\rho_M(x_1, x_2) = \beta_M (1 - x_1 - x_2)^{k-1}, \quad (6.4)$$

$$R(x_1, x_2, x) = \alpha_M \left(\frac{x_1}{x} \frac{x_2}{x}\right)^k \delta\left(1 - \frac{x_1}{x} - \frac{x_2}{x}\right)$$

and assume that $\tilde{f}_s(x_2)$ is sharply peaked near $x_2 \simeq 0$.³⁷ Under the approximation $f_s(x_2) \simeq f_s(0)$ (= const) in the integrand, $D(x, \xi)$ in (6.3) can be written as

$$D(x, \xi) = \alpha_M \beta_M \tilde{f}_s(0) (1-x)^{k-1} \left(\frac{x}{\xi}\right)^{-2k} \times \int_0^1 d\xi \tilde{F}(\xi) \left(\frac{x}{\xi} - \xi\right)^{k-1}. \quad (6.5)$$

Thus $k=1$, owing to the decay-function interpretation. That is, the counting-rule result $k=1$ is nothing but the consistency condition between the pictures of quark recombination and decay of the dressed valence quark. Also this value is compatible with the one obtained in Ref. 36 by phenomenological analysis of the kaon distributions in the fragmentation regions of the pion and the proton.

The dressed-quark decay function constructed from the recombination picture now has the form

$$D(z) = 2\alpha_M \beta_M \tilde{f}_s(0) z^{-2} \int_0^1 dx \tilde{f}_v(x), \quad (6.6)$$

where use has been made of the relation

$$\frac{1}{2} \int_0^1 dx \tilde{F}(x) = \int_0^1 dx \tilde{f}_v(x),$$

an immediate consequence of (2.2). The small- z behavior of (6.6) is obviously wrong, but it should not be taken seriously because their recombination model is expected to be reliable only in the large- x region. More importantly, the significant feature of (6.6) is that the decay function approaches a finite constant as $z \rightarrow 1$. This property, which is characteristic of the Field-Feynman decay function,²⁷ is due to the quark-recombination mechanism.³⁸

We estimate this constant by performing the analysis of the kaon spectrum with the same quark distributions $\tilde{f}_v(x) = c_\pi(1-x)^k$ and $\tilde{f}_s(x) = c_{\bar{q}}(1-x)^{n_{\bar{q}}}$ as in Ref. 36 but with $k=1$. We obtain

$$\lim_{z \rightarrow 1} D(z) = \alpha_M \beta_M c_\pi c_{\bar{q}},$$

$$\simeq \begin{cases} 0.14 & \text{for } n_{\bar{q}} = 6, \\ 0.19 & \text{for } n_{\bar{q}} = 8. \end{cases} \quad (6.7)$$

We expect that half of the above value is retained in our decay function; half is due to the characteristic feature of our model which contains only the recombination of valence and sea quarks, both of them being children of the same parent. On the other hand, in the Field-Feynman decay function²⁷

$$\lim_{z \rightarrow 1} D_{u \rightarrow K^+}(z) \simeq 0.023. \quad (6.8)$$

This is about a quarter of the expected value.

Thus we have shown, at least in the qualitative level, that the quark-recombination mechanism has been incorporated into our picture of dressed-quark decay.

VII. CONCLUSION AND DISCUSSION

In this paper we have presented a consistent description of small- p_\perp nondiffractive particle production based on

- (i) A parton-model interpretation of the QCD-inspired multijet viewpoint,
- (ii) The universality of quark-jet hadronization, and
- (iii) Correspondence arguments to dual-Regge models.

It has been shown that our model can reproduce quite well the experimental data on the following quantities without any adjustable parameters:

- (a) The average multiplicities in e^+e^- and proton-antiproton annihilations (Sec. III).
- (b) The π^\pm and K^\pm distributions in the fragmentation regions of π^\pm and K^\pm (Sec. IV).

(c) The π^+ distributions in $\bar{p}p$ annihilation, despite the fact that the agreement is not so good for favored-charge pions (Sec. V).

One of the salient features of our model is that the dressed quarks which saturate the whole momentum of hadron behave rather asymmetrically, one fast and the others slow. It is a natural consequence of the requirement that our parton description should have a good correspondence to the dual-Regge models.

Another point which we would like to emphasize is that the quark-recombination mechanism is incorporated into our dressed-quark decay as a (nonzero) finite value of the decay function $D(z)$ at $z \rightarrow 1$.

Of course it is more important to look for a crucial test of the multijet picture without entering into the details of specific models. In addition to previously proposed ones,^{3,39} we wish to call attention to the charge transfer.

The generating functional $F^{(N)}(s, h(p))$ for N -sheet processes can be written in an analogous form as in (3.1). If we restrict ourselves to the central region (c.m. rapidity ≈ 0), all the sheets may overlap with a high probability. Therefore, the effect of energy-momentum partition can be neglected. That is,

$$F^{(N)}(s, h(p)) \approx [F^{(1)}(s/N^2, h(p))]^N. \quad (7.1)$$

Using the standard technique,⁴⁰ one can show that the squared dispersion of the charge-transfer distribution of N -sheet processes is N times as large as that of one-sheet processes. Thus we expect that the charge transfer is a sensitive measure to discriminate the multijet viewpoint from the universal one-sheet picture.^{8,11}

After the completion of this work, we became aware of the paper by Capella, Sukhatme, Tan, and Trần Thanh Vân⁴¹ in which a similar model is treated. They also use a quark distribution with asymmetric configuration but without any theoretical justification. The subject of the discussion in their paper is different from ours and there is little overlap between them.

ACKNOWLEDGMENTS

I thank Dr. K. Hagiwara and Dr. K. Kanai for their useful collaboration in the very early stage of this work, and for their kind permission to use the result of their analysis of the contribution from pion diffraction. I am grateful to Professor T. Kobayashi for a careful reading of the manuscript. The numerical calculation was carried out at the Computer Center, University of Tokyo under support by the Theory Division, Institute for Nuclear Study.

*Present address: Fermi National Accelerator Laboratory, P. O. Box 500, Batavia, Illinois 60510.

¹R. P. Feynman, *Photon-Hadron Interactions* (Benjamin, New York, 1972).

²H. D. Politzer, in *Proceedings of the 19th International Conference on High Energy Physics, Tokyo, 1978*, edited by S. Homma, M. Kawaguchi, and H. Miyazawa (Physical Society of Japan, Tokyo, 1979), p. 229, and references cited therein.

³G. Veneziano, Nucl. Phys. **B117**, 519 (1976); in *Color Symmetry and Quark Confinement*, proceedings of the XII Rencontre de Moriond, Flaine, 1977, edited by J. Thanh Vân (Editions Frontières, Paris, 1977), Vol. III, p. 113; CERN Report No. Ref. TH. 2425, 1977 (unpublished).

⁴G. 't Hooft, Nucl. Phys. **B72**, 461 (1974).

⁵H. M. Chan and S. T. Tsou, Rutherford Laboratory Report No. RL-76-080, 1976 (unpublished); G. F. Chew and C. Rosenzweig, Phys. Rep. **41C**, 263 (1978).

⁶J. Kogut and L. Susskind, Phys. Rep. **8C**, 75 (1973); Z. F. Ezawa, J. Maharana, and H. Miyazawa, Prog. Theor. Phys. **51**, 877 (1974); L. Van Hove and S. Pokorski, Nucl. Phys. **B86**, 243 (1975).

⁷J. D. Bjorken and J. Kogut, Phys. Rev. D **8**, 1341 (1973).

⁸S. J. Brodsky and J. F. Gunion, Phys. Rev. Lett. **37**, 402 (1976).

⁹W. Ochs, Nucl. Phys. **B118**, 397 (1977).

¹⁰K. P. Das and R. C. Hwa, Phys. Lett. **68B**, 459

(1977). See Also, D. W. Duke and F. E. Taylor, Phys. Rev. D **17**, 1788 (1978).

¹¹B. Andersson, G. Gustafson, and C. Peterson, Phys. Lett. **69B**, 221 (1977); **71B**, 337 (1977).

¹²H. Fukuda and C. Iso, Prog. Theor. Phys. **57**, 463 (1977); **57**, 1663 (1977).

¹³K. Kinoshita, H. Noda, T. Tashiro, and M. Mizouchi, Prog. Theor. Phys. **61**, 191 (1979).

¹⁴In order to avoid confusion, we use the term "sheet" instead of "jet" in our context. A jet in the usual terminology of hard scattering is therefore "half" of a sheet.

¹⁵G. Altarelli, N. Cabibbo, L. Maiani, and R. Petronzio, Nucl. Phys. **B69**, 531 (1974); T. Kanki, Prog. Theor. Phys. **56**, 1885 (1976).

¹⁶G. Parisi and R. Petronzio, Phys. Lett. **62B**, 331 (1976); F. Martin, SLAC Report No. SLAC-PUB-2192, 1978 (unpublished), and references cited therein.

¹⁷J. Kogut and L. Susskind, Phys. Rev. D **9**, 697 (1974); **9**, 3391 (1974); G. Altarelli and G. Parisi, Nucl. Phys. **B126**, 298 (1977).

¹⁸S. J. Brodsky and J. F. Gunion, Phys. Rev. D **17**, 848 (1978).

¹⁹We do not require that the fragmentation functions of sea quarks and gluons have a power form. This is reasonable, e.g., in the valence-quark approximation (Ref. 16) where the mechanism of generation of sea quarks and gluons is quite different from the one of

- valence quarks.
- ²⁰R. D. Field and R. P. Feynman, Phys. Rev. D 15, 2590 (1977).
- ²¹S. J. Brodsky and G. Farrar, Phys. Rev. D 11, 1309 (1975); R. Blankenbecler and S. J. Brodsky, *ibid.* 10, 2973 (1974).
- ²²C. B. Chiu and S. Matsuda, Nucl. Phys. B134, 463 (1978).
- ²³H. Minakata, Tokyo Metropolitan University Report No. TMUP-HEL-807, 1978 (unpublished).
- ²⁴A. Casher, J. Kogut, and L. Susskind, Phys. Rev. D 10, 732 (1974).
- ²⁵H. Satz, invited talk at the 1977 European Conference on Particle Physics, Budapest (unpublished); Bielefeld Report No. BI-TP 77/2b, 1977 (unpublished).
- ²⁶V. Lüth, in Proceedings of the 1977 SLAC Summer Institute, SLAC Report No. 204, 1977 (unpublished). We use the data without subtracting the heavy-lepton and/or the charmed-quark effects, since it inevitably introduces certain ambiguities. They do not seem to alter our conclusion qualitatively.
- ²⁷R. D. Field and R. P. Feynman, Nucl. Phys. B136, 1 (1978).
- ²⁸In this paper the term "fragmentation region of a " implies only the forward hemisphere of particle a including the so-called pionization component.
- ²⁹J. Whitmore, Phys. Rep. 27C, 188 (1976).
- ³⁰D. Cutts *et al.*, contributed paper No. 413 to XIX International Conference on High-Energy Physics, Tokyo, 1978 (unpublished).
- ³¹Fermilab Single Arm Spectrometer Group, Phys. Rev. Lett. 35, 1195 (1975).
- ³²K. Hagiwara and K. Kanai, Tokyo Metropolitan University Report No. TMUP-HEL-806, 1978 (unpublished).
- ³³M. Barth *et al.*, contributed paper No. 1059 to the XIX International Conference on High Energy Physics, Tokyo, 1978 (unpublished).
- ³⁴P.-D. Gall, Ph.D. thesis, University of Hamburg, 1976, DESY Report No. F1-76/02, 1976 (unpublished); see also J. G. Rushbrooke and B. R. Webber, Phys. Rep. 44C, 1 (1978).
- ³⁵J. Whitmore *et al.*, Phys. Rev. Lett. 38, 996 (1977).
- ³⁶R. C. Hwa and R. G. Roberts, Rutherford Laboratory Report No. RL-78-078, 1978 (unpublished).
- ³⁷Under this assumption, the lower limit of integration in (6.2) can safely be replaced by x .
- ³⁸The fact that $D(z)$ in (6.6) depends on the sea-quark distribution does not necessarily contradict the universality of quark decay functions. This is because the "sea-quark distribution" \tilde{f}_s in the recombination model is an *effective* one as noted in Ref. 36.
- ³⁹A. Giovannini and G. Veneziano, Nucl. Phys. B130, 61 (1977).
- ⁴⁰R. Baier and F. W. Bopp, Nucl. Phys. B79, 344 (1974).
- ⁴¹A. Capella, U. Sukhatme, C.-I. Tan, and J. Trân Thanh Vân, Phys. Lett. 81B, 68 (1979).